Molecular Vision 2014; 20:732-741 <http://www.molvis.org/molvis/v20/732>
Received 19 September 2013 | Accepted 30 May 2014 | Published 2 June 2014

Downregulation of Connexin 43 promotes vascular cell loss and excess permeability associated with the development of vascular lesions in the diabetic retina

Thomas Tien, Tetsuya Muto, Kevin Barrette, Lucky Challyandra, Sayon Roy

Departments of Medicine and Ophthalmology, Boston University School of Medicine, Boston, MA

Purpose: To determine whether downregulation of Connexin 43 (Cx43) expression promotes development of acellular capillaries (ACs), pericyte loss (PL), excess permeability, and retinal thickening in rat retinas.
Methods: Control rats, diabetic rats, and rats intravitreally injected with Cx43 siRNA or scrambled siRNA were used in this study to determine if acute downregulation of Cx43 expression contributes to retinal vascular cell death and excess permeability. Western blot (WB) analysis and Cx43 immunostaining were performed to assess Cx43 protein levels and distribution in the retinal vessels. Concurrently, retinal networks were subjected to terminal deoxynucleotidyl transferase-mediated uridine 5′-triphosphate-biotin nick end labeling (TUNEL) assay and counter-stained to assess the number of apoptotic cells, ACs, and PL. Assessment of fluorescein isothiocyanate-dextran (FITC-dex) extravasation from retinal capillaries and optical coherence tomography (OCT) were performed to determine retinal vascular permeability and retinal thickness, respectively.
Results: WB analysis indicated a significant decrease in the Cx43 protein level in the retinas of the diabetic rats and those intravitreally injected with Cx43 siRNA compared to the retinas of the control rats. Likewise, the retinal vascular cells of the diabetic rats and the Cx43 siRNA-treated rats showed a significant decrease in Cx43 immunostaining. Importantly, the number of apoptotic cells, ACs and PL, FITC-dex extravasation, and thickness increased in the retinas of the diabetic and Cx43 siRNA-treated rats compared to those of the control rats.
Conclusions: Results indicate that downregulation of Cx43 expression alone induces vascular cell death and promotes vascular permeability in the retina. These findings suggest that diabetes-induced downregulation of Cx43 participates in promoting retinal vascular lesions associated with diabetic retinopathy (DR).

The development of diabetic retinopathy (DR) relies on mechanisms of early breakdown of retinal vascular homeostasis. The involvement of gap junction intercellular communication (GJIC) plays a critical role in maintaining retinal vascular homeostasis. GJIC activity is essential for maintaining tissue homeostasis and is thus a critical factor for regulating cell growth and cell death [1]. In the retina, Connexin 43 (Cx43) is abundantly present [2], which suggests a substantial amount of gap junction coupling [1,3,4]. Since high glucose (HG) downregulates Cx43 expression in retinal endothelial cells, reduced Cx43 expression could compromise cell–cell communication in the retina. Although the role of gap junction intercellular communication has been extensively studied in various tissues [5-9], its involvement with cell death via apoptosis in retinal vascular cells is only beginning to be understood.

Our previous studies have indicated that diabetes induces downregulation of Cx43 protein levels in retinal vascular cells [5,10] and that knockdown of Cx43 expression in Cx43 +/− mice promotes increased acellular capillaries (ACs) and pericyte loss (PL) in the retinal capillary network [10]. We have also observed a novel inhibitory effect of reduced Cx43 expression on cell survival, suggesting that cell–cell communication may be altered from inadequate Cx43 expression and contribute to apoptosis [11]. Therefore, HG (diabetes)-induced reduction in Cx43 expression can induce cell demise by a mechanism involving compromised cell–cell communication and result in the development of retinal vascular lesions characteristic of diabetic retinopathy. Although these findings suggest that downregulation of Cx43 expression triggers apoptosis in retinal vascular cells in vitro and in Cx43 knockout (KO) mice, it is unknown if developmental changes brought about by Cx43 downregulation contribute to apoptosis. Thus, using an siRNA strategy, the effects of direct downregulation of Cx43 on apoptosis were investigated.

An early functional change associated with the retinal vasculature in diabetic retinopathy is the breakdown of the blood–retinal barrier (BRB) [12], which is manifested throughout the progression of this ocular complication [13]. The mechanism underlying excess vascular permeability in

Correspondence to: Sayon Roy, Departments of Medicine and Ophthalmology, Boston University School of Medicine. 650 Albany Street, Boston, MA 02118; Phone: (617) 638-4110, FAX: (617) 638-4177, email: sayon@bu.edu

diabetic retinopathy is not well understood. It is clear that although tight junctions play a major role in regulating the permeability of macromolecules, recent studies indicate that gap junctions may be involved in this process. Work by Nagasawa et al. has shown the possible involvement of gap junctions in the barrier function of tight junctions of brain and lung endothelial cells [14]. Furthermore, another study showed Cx43 participates in regulating blood–testis barrier dynamics [15]. Although these studies indicate that Cx43 plays a prominent role in maintaining blood barrier characteristics, the role of Cx43 in permeability changes associated with DR is not well understood. In this study, we examined whether directly inhibiting Cx43 expression in rat retinas using intravitreally delivered Cx43 siRNA would induce changes characteristic of DR including apoptosis and increased vascular permeability.

METHODS

Streptozotocin-induced diabetic rats and Cx43 siRNA intravitreal injection: In this study, all experiments were performed in compliance with the ARVO Statement for the Use of Animals in Ophthalmic and Vision Research and approved by the IACUC regulations at Boston University School of Medicine. Thirty-two male Sprague Dawley rats were randomly assigned to four groups: normal, diabetic, normal injected with Cx43 siRNA, and normal injected with scrambled siRNA. Diabetes was induced by intraperitoneal injection with streptozotocin (STZ) at a dose of 55 mg/kg [12]. A dose of 3 µM Cx43 siRNA was intravitreally injected to achieve approximately 40% Cx43 downregulation similar to the Cx43 level in the diabetic rodent retinas. The Cx43 siRNA contained a pool of three siRNA duplexes (5′-CUG GGU CCU UCA GAU CAU Att-3′, 5′-CUG AGA ACC UAC AUC AUC Att-3′, and 5′-CUC UCG CUU UGA ACA UCA Utt-3′) targeted against the rat Cx43 transcript. Cx43 siRNA or scrambled siRNA, used as control, was administered intravitreally every 6 weeks for a total of three injections. Intravitreal injections were performed behind the ora serrata in the pars plana, directly into the vitreal cavity. Intravitreal injections were performed at an acute angle of about 30°, with a 30 gauge needle. The penetrance of the needle during the intravitreal injection was about 1 mm. Ten microliters of freshly prepared 3 µM siRNA were injected in both eyes. In parallel, rats made diabetic were maintained for 18 weeks. At the end of the study, all animals were euthanized in a chamber allowing CO_2 inhalation. No untoward effects were noted from the intravitreal injections in any of the eyes, as there was no redness or opacity as determined through routine eye examinations, as previously tested [16]. One eye from each animal was used for western blot analysis to determine the Cx43 protein level, while the contralateral eye was subjected to retinal trypsin digestion (RTD) [17] to isolate the retinal vasculature or used for retinal whole mounts. These isolated retinal vasculatures were then stained with hematoxylin and periodic acid-Schiff (PAS) and were analyzed for retinal vascular lesions. Extravasation of fluorescein isothiocyanate-dextran (FITC-dex) from retinal capillaries [13] was assessed in retinal whole mounts to determine vascular permeability. The bodyweight of the animals was routinely monitored, and at the end of the study, cardiac blood samples from these animals were assessed for HbA1c levels using the A1cNow kit (Bayer, Whippany, NJ). Insulin injections were administered in diabetic rats as required to maintain bodyweight and avoid ketoacidosis.

Western blot analysis: Western blot analysis was performed to determine the relative levels of Cx43 protein in the rat retinas from each group. Briefly, retinas were dissected from the enucleated eyes and placed in a buffer containing 25 mM Tris (pH 7.4), 1 mM EDTA, and 0.1% Triton X-100. Retinal samples were homogenized, and protein was isolated as previously described [13]. Bicinchoninic acid assay (Pierce Chemical, Rockford, IL) was used to determine the total protein concentrations. Western blot analysis was performed with 15 µg protein/lane; after electrophoresis, the gels were transferred onto polyvinyl difluoride (PVDF) membranes (Bio-Rad, Hercules, CA) using a semidry apparatus according to Towbin's procedure (electrophoretic transfer of proteins from polyacrylamide gels to nitrocellulose sheets: procedure and some applications). The membranes were blocked with 5% nonfat dry milk for 2 h and then exposed to rabbit anti-Cx43 antibody (Cell Signaling, Danvers, MA) solution (1:1,000) or rabbit anticleaved caspase-3 antibody (Cell Signaling) solution (1:600) overnight at 4 °C. Blots were washed with Tris-buffered saline containing 0.1% Tween-20 and then incubated with anti-rabbit immunoglobulin G (IgG) secondary antibody conjugated with alkaline phosphatase (Cell Signaling) solution (1:3,000) for 1 h. The membranes were again washed as described and then exposed (Immun-Star Chemiluminescent Protein Detection System; Bio-Rad) to detect the protein signals on X-ray film (Fujifilm, Tokyo, Japan). Protein loading in the gels was confirmed with Ponceau-S staining and β-actin antibody binding. The densitometric values of the Ponceau-S-stained membranes and the β-actin signals were used to correct for the western blot signals. The western blot membranes exposed to the Cx43 antibody were stripped with a buffer containing 62.5 mM Tris, pH 6.8, 2% sodium dodecyl sulfate (SDS), and 100 mM 2-mercaptoethanol and were reused with the β-actin antibody (A5060; Sigma; 1:2,500). After washing, the membranes were incubated with

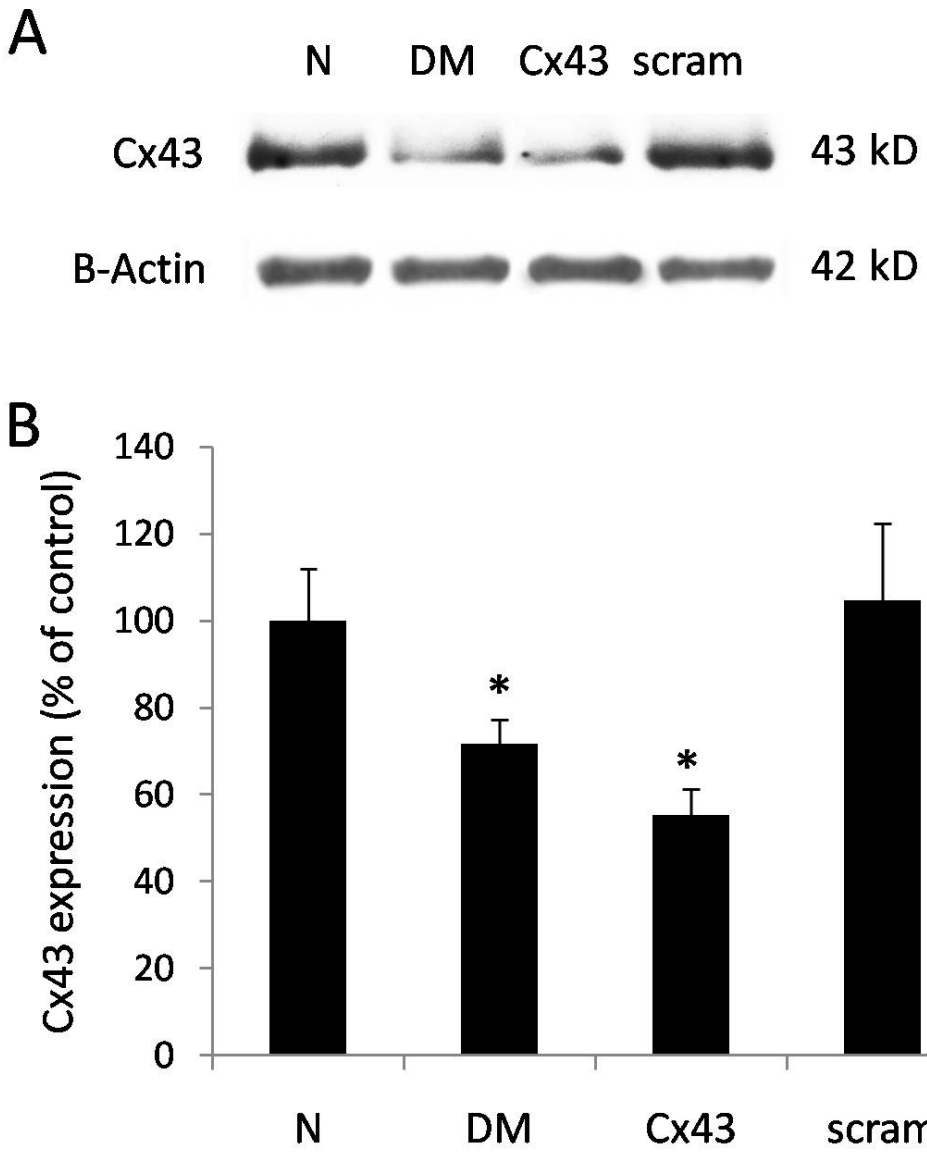

Figure 1. Cx43 protein levels in diabetic rat retinas and rats intravitreally injected with Cx43 siRNA. **A**: Representative western blot (WB) showing the Cx43 protein level in the retinas of the control rats, diabetic rats, and rats treated with intravitreal injections of Cx43 siRNA or scrambled siRNA. Corresponding β-actin protein levels show an equal amount of protein loaded in each lane (bottom). **B**: The graph shows retinal Cx43 protein levels are significantly reduced in the diabetic and Cx43 siRNA-injected rats compared to those of the controls. Data are presented as mean ± SD (* $p<0.05$, n=4).

the secondary antibody as described for Cx43 antibody detection. Densitometric analysis of the western blot signals was performed at nonsaturating exposures and analyzed using ImageJ software (developed by Wayne Rasband, National Institutes of Health, Bethesda, MD).

Retinal trypsin digestion: To analyze the retinal vasculature for ACs and PL, the RTD technique was performed as described [17], with slight modifications. Briefly, the retinas were dissected from the enucleated eyes and subjected to 3% trypsin digestion (Becton-Dickinson, San Jose, CA) at 37 °C for approximately 3 h with gentle shaking. Under a dissecting microscope, the nonvascular mass of the retina was removed from the vascular network, which was then mounted on a silane-coated slide.

Immunostaining for Cx43 and analysis of retinal trypsin digestion: To study the distribution of Cx43 gap junctions in the retinal capillaries, immunostaining was performed in the RTD preparations with Cx43 antibodies. Briefly, the RTD preparations were blocked for 15 min in 2% bovine serum albumin (BSA) to prevent nonspecific antibody binding, and then were incubated overnight at 4 °C in a moist chamber using mouse monoclonal anti-Cx43 antibody (1:100 dilution with 2% BSA; Millipore, Billerica, MA). After the overnight incubation, the RTD preparations were washed in PBS (1X; 137 mM NaCl, 2.7 mM KCl, 10 mM Na_2PO_4, 1.8 mM KH_2PO_4, pH 7.4) and incubated at room temperature with rhodamine-conjugated rabbit anti-mouse IgG secondary antibody (1:100 dilution with 2% BSA) for 1 h (Jackson

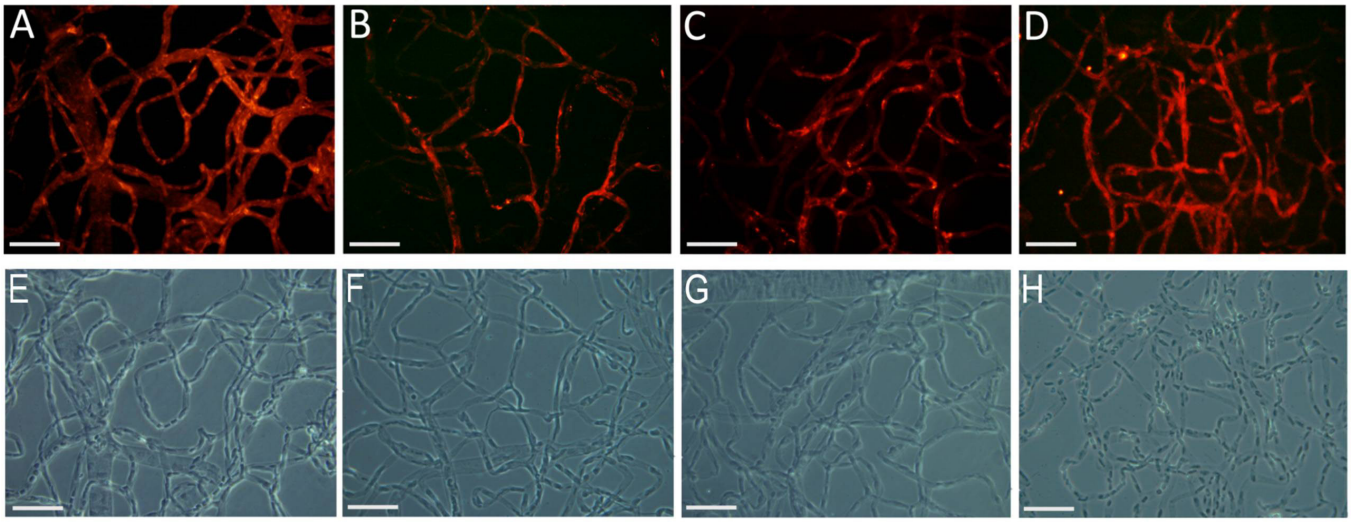

Figure 2. Cx43 immunostaining rat retinal capillaries. Representative images showing Cx43 immunostaining in the retinal vessels of (**A**) non-diabetic control rats, (**B**) diabetic rats, (**C**) non-diabetic rats intravitreally injected with Cx43 siRNA and (**D**) non-diabetic rats intravitreally injected with scrambled siRNA with corresponding bright-field images (**E**–**H**). Cx43 immunostaining was significantly reduced in the retinal vessels of diabetic rats and those of rats injected with Cx43 siRNA compared with the control rats. Images were captured at 800 ms exposure. Scale bar = 50 µm.

ImmunoResearch, West Grove, PA). After three PBS washes, the RTD preparations were mounted in reagent (SlowFade; Molecular Probes, Eugene, OR), digital images were captured at 800 ms exposure, and Cx43 immunostaining was quantified from ten random representative fields from each RTD preparation.

Detection of acellular capillaries and pericyte loss: To analyze ACs and PL, RTD preparations representing the three groups of rats were stained with PAS and Harris hematoxylin (Sigma-Aldrich, St. Louis, MO). The RTD slides were immersed in 0.5% PAS (Sigma-Aldrich) for 10 min, rinsed in dH_2O, and exposed to Schiff's reagent (Electron Microscopy Sciences, Hatfield, PA) as previously described [10]. Next, the slides were rinsed in dH_2O and immersed in Harris hematoxylin (Sigma-Aldrich) for 20 s. After rinsing in dH_2O, the slides were subjected to dehydration through an ethanol gradient and clearing in xylene and then were mounted in mounting medium (Permount; Fisher Scientific, Pittsburgh, PA). Ten representative 36 µm × 27 µm images were photographed using a digital camera (DS-Fi1; Nikon, Tokyo, Japan) connected to a computer, and the images were analyzed for ACs and PL. Apoptotic pericytes were identified as PL (pericyte ghosts) based on prominent histological characteristics, including basement membrane protrusion as an empty shell. Capillaries devoid of pericytes and endothelial cells were considered ACs. Counts were also scored by a second independent examiner in a masked manner. The data represent the average of both scores.

Terminal dUTP nick-end labeling: To determine apoptosis, terminal deoxynucleotidyl transferase-mediated uridine 5′-triphosphate-biotin nick end labeling (TUNEL) assay was performed on RTD slides representing all three experimental groups with a commercial kit (ApopTag In Situ Apoptosis Detection; Chemicon, Temecula, CA) according to the manufacturer's instructions as previously described [11]. Briefly, the RTD preparations were permeated with a precooled mixture of a 2:1 ratio of ethanol/acetic acid. After two washes in 1× PBS, slides were incubated with equilibration buffer and incubated with TdT enzyme in a moist chamber at 37 °C for 1 h. The slides were then washed with 1× PBS and incubated with anti-digoxigenin peroxidase. Finally, the slides were washed in 1× PBS and mounted using reagent (SlowFade; Molecular Probes). Images from ten random fields representing each RTD were captured using a digital microscope (DS-Fi1; Nikon) and recorded for analysis.

Retinal vasculature permeability assessment: To measure BRB permeability, we followed our method as described previously with minor modifications [13]. Briefly, tail vein injections were performed with 50 mg/kg FITC-BSA in rats from the control group and all experimental groups. After the injection, the animals were euthanized in a chamber allowing CO_2 inhalation, and the eyes were enucleated and immediately placed in 10% formaldehyde. At the time of death, blood was collected and the plasma assayed for fluorescence. Retinal whole mounts were prepared from one retina from each animal, and the pattern of vascular leakage

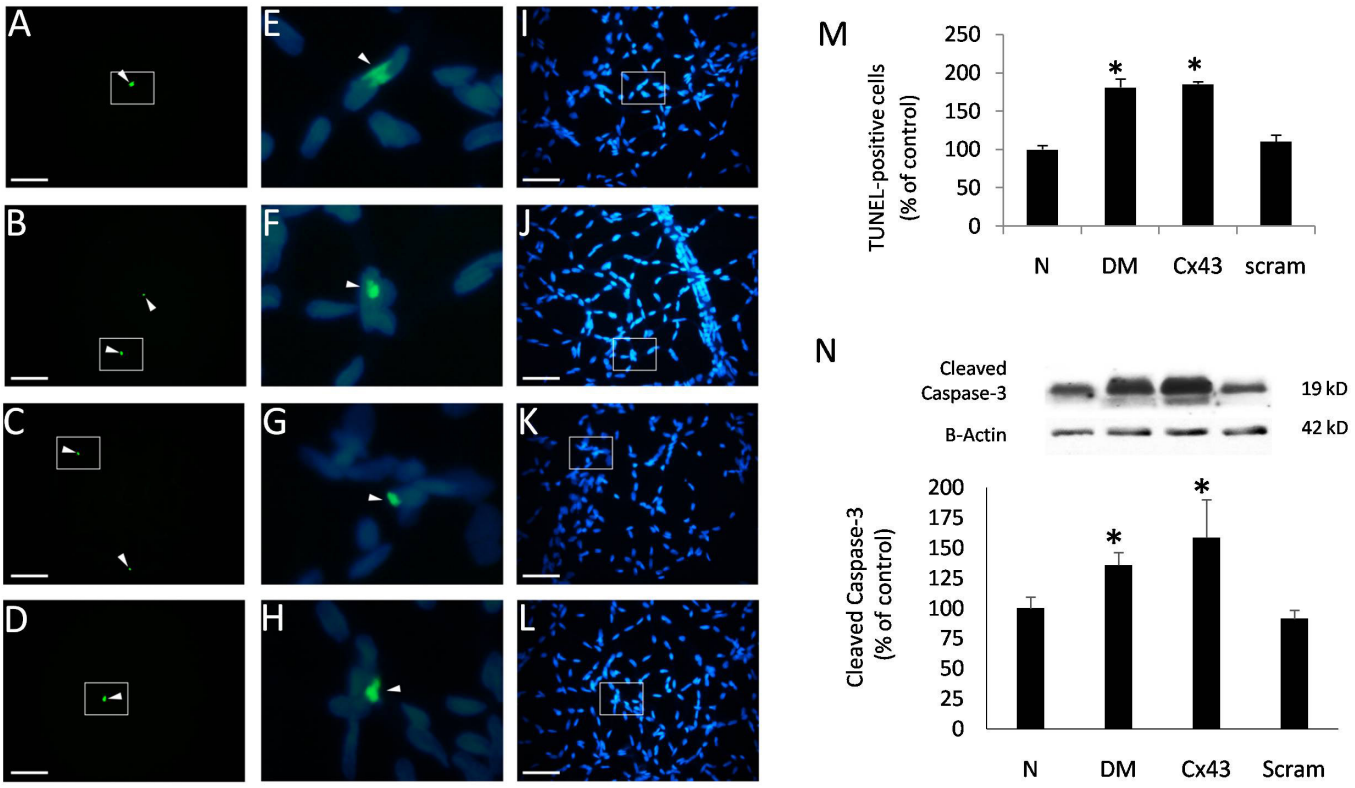

Figure 3. Cx43 downregulation promotes apoptotic death of vascular cells in the retinal capillary networks. Representative images of capillary networks showing terminal deoxynucleotidyl transferase-mediated uridine 5′-triphosphate-biotin nick end labeling (TUNEL)-positive cells in the (**A**) control rats, (**B**) diabetic rats, (**C**) rats intravitreally injected with Cx43 siRNA, and (**D**) rats intravitreally injected with scrambled siRNA. Corresponding images of the 4',6-diamidino-2-phenylindole dihydrochloride (DAPI)-stained capillary network in (**I**–**L**), respectively. The area bound by the dotted line indicates the magnified field of the DAPI-stained capillary network with a superimposed image from the TUNEL assay (**E**–**H**). An increased number of TUNEL-positive cells was present in the retinal capillary networks of the diabetic and Cx43 siRNA-injected eyes compared with the control groups. **M**: The graph presents cumulative data showing an increased number of TUNEL-positive cells in the retinal capillaries of the diabetic rats and the rats intravitreally injected with Cx43 siRNA compared with the control rats. Data are presented as mean ± SD (*p<0.05, n=4). Protein levels of cleaved caspase-3 in the rat retinas of the diabetic rats and those intravitreally injected with Cx43 siRNA. **N**: Representative western blot (WB) showing expression of cleaved caspase-3 (upper) in the retinal tissue of normal rats, diabetic rats, and rats intravitreally injected with Cx43 siRNA or scrambled siRNA. β-actin was used as the loading control (lower). The graph shows the retinal protein levels of cleaved caspase-3 are significantly increased in diabetic and Cx43 siRNA-injected rats compared to those of controls. * p<0.05. Scale bar = 50 µm.

was observed under a fluorescence microscope. The average retinal fluorescence intensity was normalized to the plasma fluorescence intensity of each animal taken at the time of death. Data are shown as mean times area divided by plasma fluorescence intensity. Areas of extravasation in the retinal whole mounts were assessed using NIH Image Analysis.

Optical coherence tomography imaging and assessment of rat retinal thickness: A high-speed spectral domain optical coherence tomography (SD-OCT) system (RTVue-100, Optovue, Fremont, CA) was used for imaging the rat retina and monitoring retinal thickness at the 2- and 3-month time points of the study. The z-axis motor drive of this device was slightly adjusted to accommodate the small axial length (approximately 6 mm) of the rat eye. After the rat was anesthetized with a cocktail containing ketamine (52 mg/kg bodyweight; Wyeth, Overland Park, KS), xylazine (7.5 mg/kg bodyweight; Butler, Columbus, OH), and acepromazine (1.1 mg/kg bodyweight; Boehringer Ingelheim, St. Joseph, MO), dilator drops (1 drop of AK-Dilate 2.5% phenylephrine hydrochloride ophthalmic solution (Akorn, Buffalo Grove, IL) and 1 drop of 1% tropicamide (Bausch & Lomb, Tampa, FL) were applied to the eye. After 10 min, mydriasis was confirmed, and the rat was placed on a movable platform in front of the OCT scanner in a manner that aligned the animal's eye with the OCT scanner lens. The retinal scans were digitally captured from areas approximately 2 optic disc

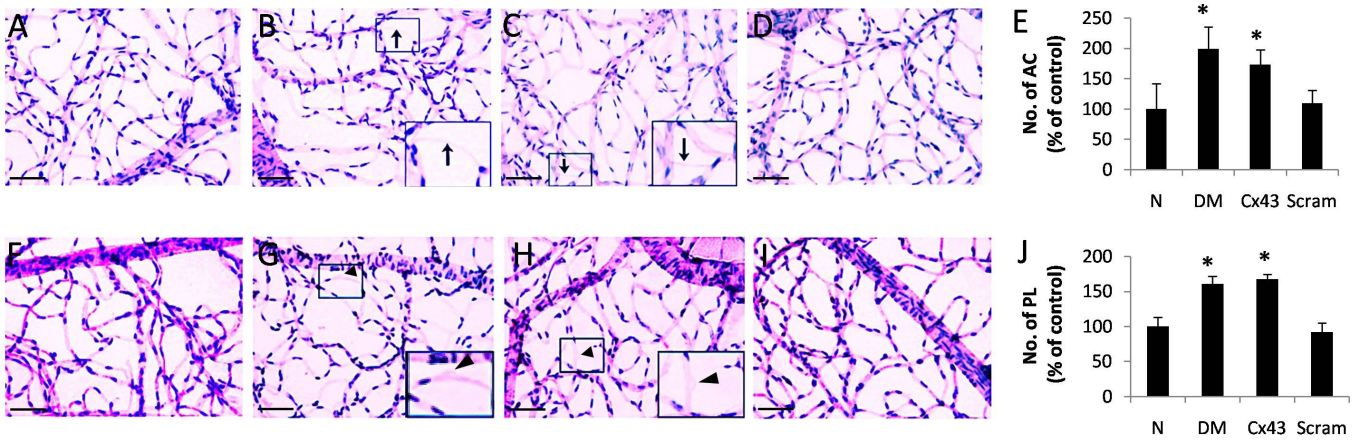

Figure 4. Cx43 downregulation promotes acellular capillary and pericyte loss in the retinal capillary networks. Representative images of the retinal capillary network stained with hematoxylin and periodic acid-Schiff showing acellular capillaries (ACs) and pericyte loss (PL) in the control rats (**A**, **F**), diabetic rats (**B**, **G**), rats intravitreally injected with Cx43 siRNA (**C**, **H**), and rats intravitreally injected with scrambled siRNA (**D**, **I**). Insets: enlarged images showing AC (long arrows) or PL (arrowheads) in the retinal trypsin digestion (RTD) preparations of the capillary networks. **E**: Percentage change in the number of ACs. The average number of ACs in the retinas of the diabetic rats and rats intravitreally injected with Cx43 siRNA was significantly increased compared with the control. * $p<0.05$. **J**: Percentage change in the amount of PL. The average amount of PL in the retinas of the diabetic rats and the rats intravitreally injected with Cx43 siRNA was significantly increased compared with that of the control rats. N, normal; DM, diabetic; Cx43, Cx43 siRNA; Scram, scrambled siRNA. Data are presented as mean ± SD (*$p<0.05$, n=4). Scale bar = 50 µm.

distance from the optic nerve head using a standard OCT scanner software that included Line, Cross-line, and E-MM5 measurements. The digital images were then assessed for retinal thickness. If a major blood vessel interrupted the image area, the average of the tissue thickness measurements from two adjacent points was used for assessment.

Statistical analysis: All data are reported as mean±standard deviation (SD); one-way ANOVA was performed followed by Tukey's post hoc test. Data with values of $p<0.05$ were considered significant.

RESULTS

Decreased Cx43 expression in retinas of diabetic rats and retinas of rats intravitreally injected with Cx43 siRNA: To determine the effects of the intravitreal injection of Cx43 siRNA in rat retinas, we performed WB analysis using total protein derived from the control and intravitreally

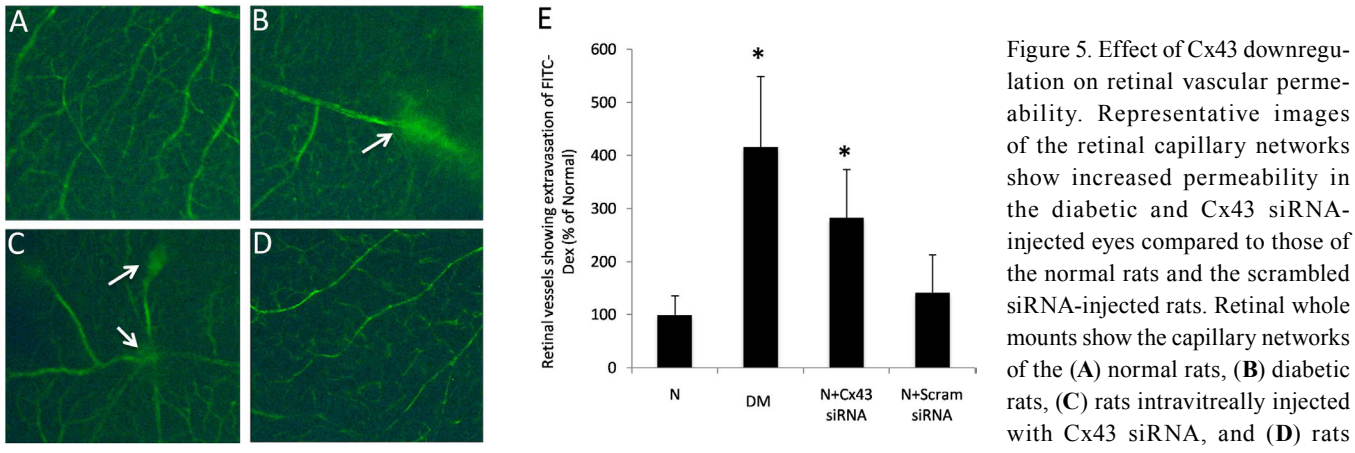

Figure 5. Effect of Cx43 downregulation on retinal vascular permeability. Representative images of the retinal capillary networks show increased permeability in the diabetic and Cx43 siRNA-injected eyes compared to those of the normal rats and the scrambled siRNA-injected rats. Retinal whole mounts show the capillary networks of the (**A**) normal rats, (**B**) diabetic rats, (**C**) rats intravitreally injected with Cx43 siRNA, and (**D**) rats intravitreally injected with scrambled siRNA. Arrows indicate areas of extravasation of fluorescein isothiocyanate-dextran in the diabetic rat retinas and those injected with Cx43 siRNA. **E**: Graphical representation of cumulative data showing a significant increase in FITC-dextran extravasation in the diabetic rats and the rats injected with Cx43 siRNA. Data are presented as mean ± SD (*$p<0.05$, n=4).

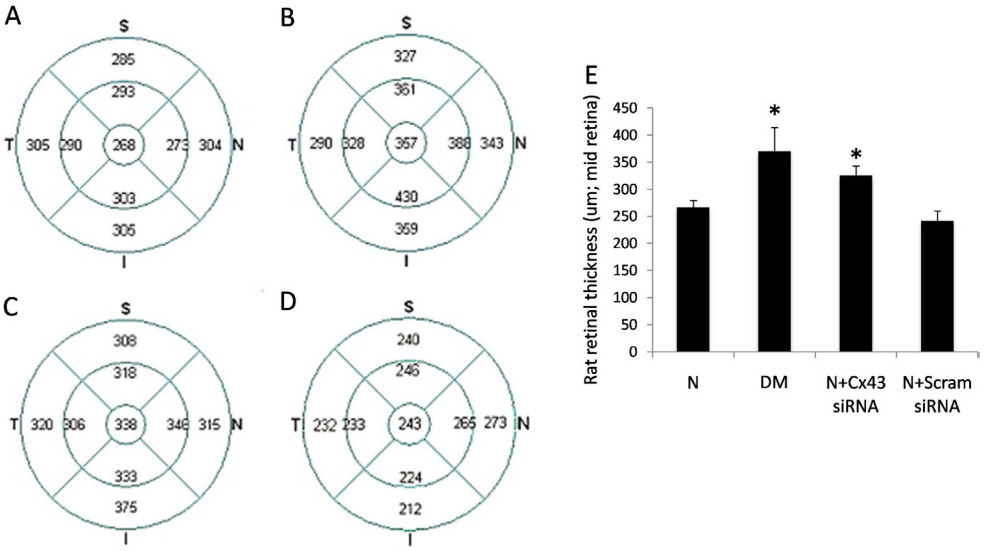

Figure 6. Effect of Cx43 downregulation on retinal thickness. Representative optical coherence tomography scans indicate increased retinal thickness in the diabetic rats and those injected with Cx43 siRNA compared to the non-diabetic or scrambled siRNA-injected control rats. Retinal thickness assessment around the midretina was made from the (**A**) non-diabetic control rats, (**B**) diabetic rats, (**C**) non-diabetic rats intravitreally injected with Cx43 siRNA, and (**D**) non-diabetic rats intravitreally injected with scrambled siRNA. Graphical illustration of cumulative data indicates significant overall thickening in the retinas of the diabetic rats and the rats injected with Cx43 siRNA compared to those of the control rats. Data are presented as mean ± SD (*p<0.05, n=4).

injected retinas. In parallel, retinas from diabetic rats were also assessed to compare the Cx43 protein level between the Cx43 siRNA-injected rats and those of the diabetic rats. The diabetic status in these animals was confirmed through HbA1c levels (8.1 versus 5.2). WB analysis showed the Cx43 protein levels were significantly reduced in the retinas of rats intravitreally injected with Cx43 siRNA, as with those of the diabetic rat retinas (60±6% of control, p<0.01, n = 4; 72±6% of control, p<0.01, n = 4; respectively) whereas the scrambled siRNA-injected rat retinas showed similar Cx43 protein levels compared to the non-diabetic rat retinas (104.7±17.8% of control; Figure 1).

To determine the effects of Cx43 siRNA intravitreal injections on the localization and distribution of Cx43, we performed Cx43 immunostaining on retinal capillary networks isolated from the retinas of the non-diabetic control rats, diabetic rats, non-diabetic rats intravitreally injected with Cx43 siRNA, and non-diabetic rats intravitreally injected with scrambled siRNA. The vascular cells in the retinal capillary networks showed a significant decrease in Cx43 immunostaining in the rats treated with Cx43 siRNA similar to that of the diabetic rats. Cx43 immunostaining in the retinal capillary network of the non-diabetic control rats and that of the scrambled siRNA-injected rats showed no difference (Figure 2).

Downregulation of Cx43 promotes apoptosis in rat retinas: To determine the effect of Cx43 downregulation on retinal vascular cell apoptosis, retinal capillary networks from the control and experimental groups were isolated and subjected to TUNEL assay. Results indicated a significant increase in the number of TUNEL-positive cells in the retinal vasculature of the diabetic and Cx43 siRNA-injected rats compared to those of the control rats (181±11% of control, p<0.05, n = 4; 186±3% of control, p<0.01, n = 4; respectively; Figure 3).

The effects of the intravitreal injection of Cx43 siRNA on apoptosis in rat retinas were also assessed with WB analysis using total protein derived from the control and intravitreally injected retinas. Results indicate that the protein levels of cleaved caspase-3 were significantly increased in the retinas of the rats intravitreally injected with Cx43 siRNA, as with those of the diabetic rat retinas (159±31% of control, p<0.05, n = 3; 136±11% of control, p<0.01, n = 3; respectively) whereas the scrambled siRNA-injected rat retinas showed similar Cx43 protein levels compared to the non-diabetic rat retinas (91±7% of control; Figure 3N).

Apoptotic cell death was manifested as pericyte ghosts or acellular capillaries, both of which were significantly increased in the diabetic retinas and in the retinas of eyes injected with Cx43 siRNA compared to the controls (PL: 160±11% of control, p<0.05, n = 4; 167±7% of control, p<0.05, n = 4; respectively; ACs: 199±41% of control, p<0.05, n = 4; 173±24% of control, p<0.05, n = 4; respectively; Figure 4). Eyes injected with scrambled siRNA showed no change in the number of ACs and PL compared to the retinas of the non-diabetic control rats (110±21% of control, 92±13% of control, respectively; Figure 4).

Downregulation of Cx43 promotes excess permeability and retinal thickening: To determine the effect of Cx43 downregulation on retinal vascular permeability, extravasation of FITC-dextran was assessed in the retinal capillaries following FITC-dextran injection. Digital images showing areas of FITC-dextran extravasation in the retinal capillary network were captured under fluorescence microscopy and analyzed for vascular leakage. Areas of focal leakages as well as leakage from individual vessels, which appeared blurry, indicative of the compromised blood–retinal barrier, were observed in the diabetic rats and those injected with Cx43 siRNA (Figure 5A). As expected, the retinal capillary networks of the diabetic rats showed increased vascular leakage compared to those of the non-diabetic control rats. Importantly, retinal vascular permeability was significantly increased in the rats intravitreally injected with Cx43 siRNA, whereas injection with scrambled siRNA had no effect on retinal vascular permeability. Figure 5B presents cumulative data for retinal vessels showing extravasation of FITC-dex in the experimental groups compared to the control.

To determine the consequence of excess retinal vascular permeability, we assessed retinal thickness using spectral domain OCT in the non-diabetic control rats, diabetic rats, Cx43 siRNA intravitreally injected rats, and scrambled siRNA-injected rats. Retinal thickness assessments were performed using OCT scans around the central and midretina at a distance approximately 2 optical disks from the optic nerve head (Figure 6). A significant increase in retinal thickness was observed in the rats injected with Cx43 siRNA that was comparable to the retinal thickness of the diabetic rats (Figure 6). Injections with scrambled siRNA showed no effect on retinal thickness.

DISCUSSION

The results from the present study demonstrate for the first time that downregulation of Cx43 expression alone is sufficient to induce apoptosis in the retinal vascular cells that is subsequently manifested as PL and ACs in the diabetic retina. Excess vascular permeability was observed in retinas that received intravitreal injections of Cx43 siRNA similar to that of the diabetic retinas, and importantly, the OCT scans indicated a marked thickening of the retina. These findings suggest that the decreased levels of Cx43 seen in the diabetic retina may influence vascular cell demise and contribute to blood–retinal barrier breakdown. Although neuronal tearing may play a role in altered retinal thickness, findings from our study suggest that vascular leakage is likely the major contributory factor leading to retinal thickening. Downregulation of Cx43 results in increased vascular leakage, as evidenced by increased extravasation of FITC-dextran in rats given intravitreal Cx43 siRNA injection. This result is consistent with our previous findings that Cx43 downregulation reduces the expression of tight junction proteins and increases cell monolayer permeability [18].

Cx43 downregulation in the retina by direct intravitreal delivery alone is sufficient to promote vascular cell death and excess permeability. Our previous studies examining the role of Cx43 in mediating apoptosis were performed using in vitro cell culture models and animal models of diabetes [10,11]. The in vitro cell culture model demonstrated that reduced Cx43 expression could induce apoptosis in retinal endothelial cells [11]. In both animal models, Cx43 knockout mice and diabetic rats, vascular lesions similar to those seen in diabetic retinas were observed. However, it was unclear whether the decreased level of retinal Cx43 alone, without the influence of developmental changes associated with a knockout animal system, was sufficient to induce the characteristic retinal vascular lesions. The results of the current study are consistent with our previous findings that high-glucose-induced downregulation of Cx43 may disrupt vascular homeostasis and promote vascular cell death characteristic of diabetic retinopathy. Although the exact mechanism underlying Cx43 downregulation–induced apoptosis is unclear, a study reported that Cx43 translocates to the mitochondria, where it interacts with Bax to initiate the mitochondrial apoptotic pathway [19]. Since high glucose decreases cell surface Cx43 [5,11] and mitochondrial Cx43 [20], the ensuing accumulation of cytoplasmic Cx43 could promote the mitochondrial apoptotic pathway.

The role of gap junctions in maintaining blood barrier characteristics is only beginning to be understood. Findings from the current study suggest that Cx43 downregulation may be involved in the breakdown of the blood–retinal barrier and promote vascular permeability in diabetic retinopathy. Several studies have reported that Cx43 is involved in regulating tight junction proteins associated with blood barriers, such as occludin [21,22] and zona occuldens 1 (ZO-1) [23]. It has also been suggested that gap junctions are required for the barrier functions of endothelial cells and that signaling molecules such as Ca^{2+}, IP3, and cAMP can pass through Cx43 gap junction channels and may coordinate the barrier function of tight junctions [14]. Reduction in Cx43 expression and gap junction intercellular communication may compromise the transfer of signaling molecules and adversely affect the barrier properties of endothelial cells. Furthermore, Cx43 expression was shown to play a role in homeostasis of the blood–testis barrier [15]. Sertoli cells with reduced Cx43 exhibited delayed tight junction barrier reassembly during

calcium repletion. These studies underscore the critical role of connexins in maintaining blood barrier function. Further studies are needed to identify the mechanism underlying Cx43 downregulation–induced breakdown of barrier characteristics.

Although most studies indicate that Cx43 downregulation is closely associated with the development of diabetic vascular complications, study findings have also suggested Cx43 upregulation. Cx43 downregulation by high glucose was recently shown to mediate nuclear factor-kappa B (NF-κB) signaling in glomerular mesangial cells [24]. Similarly, high glucose–induced downregulation of Cx43 and subsequent reduction of GJIC was reported to be involved in endothelial cell dysfunction associated with the breakdown of the blood–retinal barrier in diabetic retinopathy [25], decreased Cx43 expression was observed in the endothelial cells of the renal efferent arterioles of diabetic rats [26], and decreased Cx43 in smooth muscle cells was strongly associated with diabetes-related bladder dysfunction [27]. Although most studies report Cx43 downregulation in various tissues or cell types in diabetes or a high glucose condition, a study reported Cx43 overexpression in a high glucose condition in the human collecting duct cell line, and recently, Cx43 overexpression was observed in diabetic foot ulcers [28]. Thus, further studies are necessary to better understand how high glucose differentially alters Cx43 expression.

A limitation of the present study is that it focused on the effects of reduced Cx43 only on the retinal vascular cells related to the inner BRB. Therefore, further studies are needed to investigate the effects of Cx43 downregulation on the outer BRB. Decreased Cx43 levels are known to influence intercellular communication between other cell types in the retina. In particular, Müller cells that span the entire retina frequently come in contact with various retinal cell types, including astrocytes, oligodendrocytes, and pericytes, and thus, reduced Cx43 expression in Müller cells can have a profound effect on retinal homeostasis in general. Our recent studies indicated that Cx43 expression is reduced by HG in cultures of retinal Müller cells (rMC-1), and that HG-induced loss of intercellular communication in retinal Müller cells and between Müller cells and pericytes may negatively impact vascular cell viability and homeostasis [29]. Thus, decreased Cx43 in these cells can influence retinal homeostasis through compromised crosstalk that ultimately contributes to the demise of the cells and breakdown of the blood–retinal barrier. Although Cx43 deficiency has been identified as a critical mediator in several diseases, such as arrhythmias [30,31], congestive heart failure [32], and oculodentodigital dysplasia [33], among others, our current findings provide the first evidence that downregulation of Cx43 expression in the retina can promote vascular lesions characteristic of DR.

ACKNOWLEDGMENTS

Research was supported by NIH, NEI R01EY018218, and in part by a departmental grant from the Massachusetts Lions Eye Research Fund.

REFERENCES

1. De Maio A, Vega VL, Contreras JE. Gap junctions, homeostasis, and injury. J Cell Physiol 2002; 191:269-82. [PMID: 12012322].
2. Janssen-Bienhold U, Dermietzel R, Weiler R. Distribution of connexin43 immunoreactivity in the retinas of different vertebrates. J Comp Neurol 1998; 396:310-21. [PMID: 9624586].
3. Goodenough DA, Goliger JA, Paul DL. Connexins, connexons, and intercellular communication. Annu Rev Biochem 1996; 65:475-502. [PMID: 8811187].
4. Oku H, Kodama T, Sakagami K, Puro DG. Diabetes-induced disruption of gap junction pathways within the retinal microvasculature. Invest Ophthalmol Vis Sci 2001; 42:1915-20. [PMID: 11431461].
5. Sato T, Haimovici R, Kao R, Li AF, Roy S. Downregulation of connexin 43 expression by high glucose reduces gap junction activity in microvascular endothelial cells. Diabetes 2002; 51:1565-71. [PMID: 11978657].
6. Inoguchi T, Ueda F, Umeda F, Yamashita T, Nawata H. Inhibition of intercellular communication via gap junction in cultured aortic endothelial cells by elevated glucose and phorbol ester. Biochem Biophys Res Commun 1995; 208:492-7. [PMID: 7695598].
7. Zhang YW, Morita I, Nishida M, Murota SI. Involvement of tyrosine kinase in the hypoxia/reoxygenation-induced gap junctional intercellular communication abnormality in cultured human umbilical vein endothelial cells. J Cell Physiol 1999; 180:305-13. [PMID: 10430170].
8. Inoguchi T, Yu HY, Imamura M, Kakimoto M, Kuroki T, Maruyama T, Nawata H. Altered gap junction activity in cardiovascular tissues of diabetes. Med Electron Microsc 2001; 34:86-91. [PMID: 11685657].
9. Patterson CE, Lum H, Schaphorst KL, Verin AD, Garcia JG. Regulation of endothelial barrier function by the cAMP-dependent protein kinase. Endothelium 2000; 7:287-308. [PMID: 11201526].
10. Bobbie MW, Roy S, Trudeau K, Munger SJ, Simon AM. Reduced connexin 43 expression and its effect on the development of vascular lesions in retinas of diabetic mice. Invest Ophthalmol Vis Sci 2010; 51:3758-63. [PMID: 20130277].
11. Li AF, Roy S. High Glucose-Induced Downregulation of Connexin 43 Expression Promotes Apoptosis in

Microvascular Endothelial Cells. Invest Ophthalmol Vis Sci 2009; 50:1400-7. [PMID: 19029021].

12. Cherian S, Roy S, Pinheiro A. Tight glycemic control regulates fibronectin expression and basement membrane thickening in retinal and glomerular capillaries of diabetic rats. Invest Ophthalmol Vis Sci 2009; 50:943-9. [PMID: 18775856].
13. Oshitari T, Polewski P, Chadda M, Li AF, Sato T, Roy S. Effect of combined antisense oligonucleotides against high-glucose- and diabetes-induced overexpression of extracellular matrix components and increased vascular permeability. Diabetes 2006; 55:86-92. [PMID: 16380480].
14. Nagasawa K, Chiba H, Fujita H, Kojima T, Saito T, Endo T, Sawada N. Possible involvement of gap junctions in the barrier function of tight junctions of brain and lung endothelial cells. J Cell Physiol 2006; 208:123-32. [PMID: 16547974].
15. Li MW, Mruk DD, Lee WM, Cheng CY. Connexin 43 is critical to maintain the homeostasis of the blood-testis barrier via its effects on tight junction reassembly. Proc Natl Acad Sci USA 2010; 107:17998-8003. [PMID: 20921394].
16. Chronopoulos A, Trudeau K, Roy S, Huang H, Vinores SA. High glucose-induced altered basement membrane composition and structure increases trans-endothelial permeability: implications for diabetic retinopathy. Curr Eye Res 2011; 36:747-53. [PMID: 21780924].
17. Kuwabara T, Cogan DG. Studies of retinal vascular patterns. I. Normal architecture. Arch Ophthalmol 1960; 64:904-11. [PMID: 13755464].
18. Tien T, Barrette KF, Chronopoulos A, Roy S. Effects of high glucose-induced Cx43 downregulation on occludin and ZO-1 expression and tight junction barrier function in retinal endothelial cells. Invest Ophthalmol Vis Sci 2013; 54:6518-25. [PMID: 24008412].
19. Sun Y, Zhao X, Yao Y, Qi X, Yuan Y, Hu Y. Connexin 43 interacts with Bax to regulate apoptosis of pancreatic cancer through a gap junction-independent pathway. Int J Oncol 2012; 41:941-8. [PMID: 22736223].
20. Trudeau K, Muto T, Roy S. Downregulation of mitochondrial connexin 43 by high glucose triggers mitochondrial shape change and cytochrome C release in retinal endothelial cells. Invest Ophthalmol Vis Sci 2012; 53:6675-81. [PMID: 22915032].
21. Chronopoulos A, Tang A, Beglova E, Trackman PC, Roy S. High glucose increases lysyl oxidase expression and activity in retinal endothelial cells: mechanism for compromised extracellular matrix barrier function. Diabetes 2010; 59:3159-66. [PMID: 20823103].
22. Lee NP, Yeung WS, Luk JM. Junction interaction in the seminiferous epithelium: regulatory roles of connexin-based gap junction. Front Biosci 2007; 12:1552-62. [PMID: 17127402].
23. Bekheet SH, Stahlmann R. Disruption of gap junctional intercellular communication by antibiotic gentamicin is associated with aberrant localization of occludin, N-cadherin, connexin 43, and vimentin in SerW3 Sertoli cells in vitro. Environ Toxicol Pharmacol 2009; 28:155-60. [PMID: 21783997].
24. Xie X, Lan T, Chang X, Huang K, Huang J, Wang S, Chen C, Shen X, Liu P, Huang H. Connexin43 mediates NF-kappaB signalling activation induced by high glucose in GMCs: involvement of c-Src. Cell Commun Signal 2013; 11:38- [PMID: 23718910].
25. Fernandes R, Girao H, Pereira P. High glucose down-regulates intercellular communication in retinal endothelial cells by enhancing degradation of connexin 43 by a proteasome-dependent mechanism. J Biol Chem 2004; 279:27219-24. [PMID: 15123628].
26. Zhang J, Hill CE. Differential connexin expression in preglomerular and postglomerular vasculature: accentuation during diabetes. Kidney Int 2005; 68:1171-85. [PMID: 16105048].
27. Poladia DP, Schanbacher B, Wallace LJ, Bauer JA. Innervation and connexin isoform expression during diabetes-related bladder dysfunction: early structural vs. neuronal remodelling. Acta Diabetol 2005; 42:147-52. [PMID: 16258738].
28. Mendoza-Naranjo A, Cormie P, Serrano AE, Wang CM, Thrasivoulou C, Sutcliffe JE, Gilmartin DJ, Tsui J, Serena TE, Phillips AR, Becker DL. Overexpression of the gap junction protein Cx43 as found in diabetic foot ulcers can retard fibroblast migration. Cell Biol Int 2012; 36:661-7. [PMID: 22455314].
29. Muto T, Stottrup C, Roy S. Effect of High Glucose on Connexin 43 (Cx43) Expression Localization and Intercellular Communication in Retinal Muller Cells and Retinal Pericytes. 2012; 51:D846-.
30. Geisler SB, Green KJ, Isom LL, Meshinchi S, Martens JR, Delmar M, Russell MW. Ordered assembly of the adhesive and electrochemical connections within newly formed intercalated disks in primary cultures of adult rat cardiomyocytes. J Biomed Biotechnol 2010; 2010:624719-[PMID: 20467587].
31. Fontes MS, van Veen TA, de Bakker JM, van Rijen HV. Functional consequences of abnormal Cx43 expression in the heart. Biochim Biophys Acta 2012; 1818:2020-9. [PMID: 21839722].
32. Dupont E, Matsushita T, Kaba RA, Vozzi C, Coppen SR, Khan N, Kaprielian R, Yacoub MH, Severs NJ. Altered connexin expression in human congestive heart failure. J Mol Cell Cardiol 2001; 33:359-71. [PMID: 11162139].
33. Lai A, Le DN, Paznekas WA, Gifford WD, Jabs EW, Charles AC. Oculodentodigital dysplasia connexin43 mutations result in non-functional connexin hemichannels and gap junctions in C6 glioma cells. J Cell Sci 2006; 119:532-41. [PMID: 16418219].

Articles are provided courtesy of Emory University and the Zhongshan Ophthalmic Center, Sun Yat-sen University, P.R. China. The print version of this article was created on 2 June 2014. This reflects all typographical corrections and errata to the article through that date. Details of any changes may be found in the online version of the article.